Head phantoms for bioelectromagnetic applications: a material study

Alexander Hunold (alexander.hunold@tu-ilmenau.de)
Technische Universitat Ilmenau https://orcid.org/0000-0001-7315-1115
René Machts
Technische Universitat Ilmenau
Jens Haueisen
Technische Universitat Ilmenau

Research

Keywords: conductivity, anisotropy, impedance spectroscopy, EEG, TES, agar hydrogel

Posted Date: August 31st, 2020

DOI: https://doi.org/10.21203/rs.3.rs-65571/v1

Version of Record: A version of this preprint was published on November 23rd, 2020. See the published version at https://doi.org/10.1186/s12938-020-00830-y.

Abstract

Background Assessments of source reconstruction procedures in electroencephalography and computations of transcranial electrical stimulation profiles require verification and validation with the help of ground truth configurations as implemented by physical head phantoms. Phantoms provide well-defined volume conduction configurations with realistic geometries.

We aim to characterize the electrical conductivity of materials for modeling head compartments to establish reproducible and stable physical head phantoms.

We analyzed sodium chloride (NaCl) solution, agarose hydrogel, gypsum and reed sticks as surrogate materials for the intracranial volume, scalp, skull and anisotropic conductivity structures. We measured the impedance of all materials when immersed in NaCl solution using a four-point setup. The electrical conductivity values of each material were calculated from the temperature compensated impedances considering the sample geometries.

Results We obtained conductivities of 0.332 S/m (0.17 % NaCl solution), 0.0425 S/m and 0.0017 S/m (gypsum with and without NaCl), 0.314 S/m, 0.30 S/m, 0.311 S/m (2 %, 3 %, 4 % agarose). The reed sticks were tested in longitudinal and transversal direction and showed anisotropic conductivity with a ratio of 1:2.8.

Conclusion We conclude that the tested materials NaCl solution, gypsum and agarose can serve as stable representation of the three main conductivity compartments of the head, intracranial volume, skull and scalp. An anisotropic conductivity structure such as a piece of white matter can be modeled using tailored reed sticks inside a volume conductor.

Background

Technologies such as transcranial electric stimulation (TES), transcranial current density imaging (CDI) and neuronal source imaging based on electroencephalography (EEG) and magnetoencephalography (MEG), require methodologies for verification and validation. The assessment of new measurement and analysis chains can be pursued; applying (i) computational modeling and simulation [1] and (ii) metrological inspections [2, 3]. While computational modeling and simulations provide a convenient way of assessing the above technologies, only metrological inspections allow the inclusion of real-world environmental influences and can provide validation for computational modeling and simulations based on ground truth.

For EEG/MEG, the spread of electromagnetic fields caused by intracranial generators is of high importance for the identification of bio-electric sources [4]. For TES, dosage considerations require exact knowledge of the spread of the electromagnetic field inside the head [5]. In both applications, the computation of the electromagnetic field requires a thorough knowledge of the volume conductor, i.e. the 3D conductivity profile within the human head. The geometry is commonly segmented from magnetic resonance imaging data sets [6] and the conductivity values are derived from literature. The values derived from literature demonstrate a

large variation, resulting from inter- and intra-individual differences [7], different measurement methodology [8] as well as other factors, but do not necessarily represent the individual conductivity profile [7, 8].

A large part of the uncertainty in the conductivity configuration can be overcome within a physical phantom of the head as volume conductor. The geometry of the phantom is predefined by the design and manufacturing processes and the conductivity properties of the phantom materials can be measured in advance.

Considering the human head as a volume conductor, the skull provides the major conductivity barrier. Consequently, three conductivity compartments are of particular interest: scalp (soft tissue outside of the skull), skull and intracranial volume [9]. The soft tissue compartments with higher conductivity encase the skull compartment with low conductivity. A widely used conductivity value for intracranial volume is 0.33 S/m [10]. According to previous literature, the ratios for the skull-to-soft tissue conductivity ranges from 1:120 [11] to 1:5 [12]. A further feature of interest for physical representation is conductivity anisotropy, which occurs mainly in the fiber tracts of white matter. The anisotropy ratio between the longitudinal and transversal direction in white matter varied from 1:2 to 1:100 in modeling studies [13, 14] and was measured in the cat to be 1:10 [15].

Previous approaches established head phantoms based on post-mortem human skulls assessing EEG source reconstruction procedures [16, 17] or used doped saline solutions for the verification of TES simulations [18, 19]. Conductivity anisotropy in a human torso phantom was modeled by skeins built from guar gum [20]. These phantoms incorporated saline solutions with different electrolyte concentration to obtain different conductivity values. Interfacing multiple compartments based on different saline solutions introduces concentration gradients leading to diffusion processes. The time-dependent electrolyte diffusion limits the stability of the respective conductivity configurations in such phantoms.

The aim of this study is to introduce suitable synthetic materials allowing ion conduction with inherently different conductivities to model a multi-compartment phantom, representing a realistic human head geometry. Therefore, we characterize materials providing adjustable conductivity based on a constant electrolyte concentration. With the skull material, we want to achieve the main structural conductivity barrier for ions. For the implementation of the skull, we chose a material that is plastically formable during the manufacturing process, in order to replicate a real human skull geometry. This material should be mechanically stable enough to serve as a support structure for adjacent compartments. Similarly, the material for the scalp should provide mechanical stability, allowing the attachment of electrodes for measurements or stimulation. For the intracranial volume, we required a material that allows for easy insertion of structures for signal generation (dipoles) or measurement (electrodes arrays).

Results

Sodium chloride solution

A conductivity of 0.333 S/m ± 0.001 S/m (mean ± std) was measured in 0.17 % NaCl solutions with the ProfiLine Cond 3310 (0.5 % uncertainty) with a temperature compensation to 25 °C, which is in accordance

with previously published data [22]. Without temperature compensation, the 0.17 % NaCl solution provided conductivities of 0.299 S/m ± 0.005 S/m on the ProfiLine Cond 3310 at temperatures of 20.04 °C ± 0.70 °C. Considering these conductivities and the geometry with an inner electrode distance of 25 mm and a tube diameter of 58 mm, the reference impedance for 0.17 % NaCl solution for our cell configuration was 31.69 Ohm at 20 °C and 28.45 Ohm at 25 °C (Z_{25ref}). The measured impedance of the reference 0.17 % NaCl solutions in the four-point setup was 31.41 Ohm ± 0.14 Ohm (Z_{meas}) which corresponded to conductivities of 0.301 S/m ± 0.002 S/m. During these measurements, the temperature in the 0.17 % NaCl solutions was 21.04 °C ± 0.18 °C (ϑ_{meas}). Using Equation 1, we determine the cell constant α to -0.026 for the four-point setup using Z_{25ref}, Z_{meas} and ϑ_{meas} from the impedance measurements with only 0.17 % NaCl solution in the cell.

With the temperature compensation applied, the impedance of 0.17 % NaCl solution in the four-point setup was 28.39 Ohm ± 0.19 Ohm at 25 °C, resulting in a conductivity of 0.332 S/m ± 0.003 S/m. Figure 1 depicts the averaged conductivity traces from the three sample solutions with their mean and standard deviation.

Agar hydrogel

The three samples of 2 wt% agar hydrogel doped with 0.17 % NaCl solution provided a conductivity of 0.284 S/m ± 0.009 S/m at a temperature of 21.05 °C ± 0.23 °C which corresponded to a conductivity of 0.314 S/m ± 0.01 S/m at 25 °C.

The samples with 3 wt% agar provided a conductivity of 0.272 S/m ± 0.005 S/m at a temperature of 20.99 °C ± 0.19 °C which corresponded to a conductivity of 0.302 S/m ± 0.005 S/m at 25 °C.

The samples with 4 wt% agar provided a conductivity of 0.281 S/m ± 0.02 S/m at a temperature of 20.88 °C ± 0.41 °C which corresponded to a conductivity of 0.311 S/m ± 0.018 S/m at 25 °C.

Figure 2 presents the averaged conductivity data from the samples of 2 wt%, 3 wt% and 4 wt% agar in 0.17 % NaCl solution with their standard deviation, both for the frequency range and the constant frequency of 1 Hz.

Figure 3 presents the averaged conductivity data from the three samples of 2 wt% agar in 0.17 % NaCl solution with their standard deviation, both for the extended frequency range from 0.01 Hz to 100 kHz and the constant frequency of 10 Hz. In this measurement regime, the samples provided a conductivity of 0.276 S/m ± 0.006 S/m at a temperature of 20.76 °C ± 0.1 °C which corresponded to a conductivity of 0.306 S/m ± 0.007 S/m at 25 °C.Even though measurements were conducted in a grounded faraday cage, the spectra showed a deviation at 50 Hz reflecting power-line interference.

Gypsum

Figure 4 presents the conductivity data from one sample of Stewaform gypsum without NaCl in the casting compound infiltrated with epoxy resin and immersed in 0.17 % NaCl solution. The sample was repeatedly tested with at least 20 h at ambient air between measurements. Each test contained three measurement series.

Figure 5 presents the conductivity data from the sample of Stewaform gypsum with NaCl in the casting compound infiltrated with epoxy resin and immersed in 0.17 % NaCl solution. The sample was repeatedly tested with at least 20 h at ambient air between measurements. Each test contained three measurement series. Across the three measurement series, the sample provided a conductivity of 0.037 S/m ± 0.0012 S/m at a temperature of 18.85 °C ± 0.19 °C which corresponded to a conductivity of 0.043 S/m ± 0.0015 S/m at 25 °C.The gypsum sample demonstrated a capacitive character with increasing conductivity for frequencies above 1 kHz, such that the phase decreased from -8 degrees at 1 kHz to -50 degrees at 100 kHz. For quantitative evaluations, the frequency range up to 1 kHz was considered. Given the dry initial condition of the gypsum, the sample demonstrated a conductivity of 0.0008 S/m ± 0.0001 S/m at 25 °C in the first measurement series. In the following measurement series, the previously dried sample demonstrated a conductivity of 0.0017 S/m ± 0.00004 S/m at 25 °C.

Figure 6 presents the averaged conductivity data from the three samples of gypsum with NaCl in the casting compound with their standard deviation, both for the extended frequency range from 0.01 Hz to 100 kHz and the constant frequency of 10 Hz. In this measurement regime, the samples provided a conductivity of 0.037 S/m ± 0.002 S/m at a temperature of 19.75 °C ± 0.26 °C which corresponded to a conductivity of 0.042 S/m ± 0.003 S/m at 25 °C.

Conductivity anisotropy

In Figure 7 we present the conductivity data and the conductivity anisotropy ratio from a tube cell configuration holding 80 reed sticks and filled with 0.17 % NaCl solution. The setup was kept sealed during the complete measurement series. Measurements 1 and 2 were performed on the same day with a break of 6 h in between. The subsequent measurements 3 and 4 were performed on consecutive days and the last measurement 5 was performed after a break of 3 days.

The spectra again showed deviations at 50 Hz, reflecting power-line interference. The noise level was generally higher for frequencies above approximately 300 Hz.In longitudinal direction, the reed sticks provided an average conductivity of 0.32 S/m with a mean standard deviation of 0.02 S/m (6.2 %) at 10 Hz over 60 min and a mean conductivity of 0.32 S/m with a standard deviation of 0.003 S/m (0.9 %) across the tested frequency spectrum.
In transversal direction, the reed sticks provided an average conductivity of 0.12 S/m with a mean standard deviation of 0.001 S/m (0.8 %) at 10 Hz for 60 min and a mean conductivity of 0.12 S/m with a standard deviation of 0.003 S/m (2.5 %) across the tested frequency spectrum.

These conductivity differences between longitudinal and transversal direction resulted in a conductivity anisotropy ratio (mean ± standard deviation) of 2.8 ± 0.02 at 10 Hz over 1 hour and 2.7 ± 0.05 across the tested frequency range.

Discussion

In this study, we investigated the feasibility of establishing a realistically shaped multi-compartment head phantom, incorporating realistic electrolyte conductivity levels based on a 0.17% NaCl solution using agar hydrogel, gypsum and reed sticks.

The 0.17% NaCl solution demonstrated a conductivity of 0.33 S/m at 25 °C which corresponds to the value that is widely used to model the conductivity of intracranial volume [10]. Consequently, this saline solution established the fundamental electrolyte concentration that prevailed throughout all compartments. In a closed phantom design, the saline solution itself can be used to model the intracranial volume. Interior structures for signal generation (dipoles) or measurement (electrodes) can be inserted into the aqueous solution without interfering with the structure of this compartment.

Doping the NaCl solution with agarose as solidifying agent enabled the formation of a mechanically durable scalp layer. The conductivity value of the agar hydrogel decreased on average by 7% (2 wt%: 5.5%, 3 wt%: 9.0%, 4 wt%: 6.3%) compared to the pure NaCl solution. Conductivity value variations over the tested time interval and frequency interval as well as across measurement repetitions stayed well within a 5% std range. The average measured conductivity of 0.31 S/m at 25 °C was in acceptable accordance with the value of 0.435 S/m measured at 37 °C by Burger and Milaan and within the range from 0.137 S/m to 2.1 S/m summarized by McCann et al. [8, 23]. Adapting the agar concentration in the range from 2% to 4% gave the opportunity to modify its mechanical durability without changing the conductivity to an inacceptable range. With an agar concentration of 4%, applications such as EEG experiments using dry multi-pin electrodes become feasible [24].

The tested gypsum material demonstrated a considerable conductivity barrier. The two tested material configurations, with 0.17% NaCl in the casting compound and without NaCl in the casting compound, covered a wide range of skull conductivities, varying from 0.00275 S/m [11] to 0.066 S/m [12] according to literature.

After an initial soaking of the sample during the first measurement, the gypsum without NaCl in the casting compound provided stable results within a 5% std margin over the tested frequency range and time interval as well as across measurement repetitions. The measured average conductivity value of 0.0017 S/m at 25 °C for the gypsum without NaCl in the casting compound was in well accordance with skull conductivity values of 0.0038 S/m at 36.5 °C reported by Tang et al. [25].

The gypsum samples with 0.17% NaCl in the casting compound provided stable results within a 5% std margin across multiple measurement series and a reproducibility of multiple samples within a 10% std margin. The measured average conductivity value of 0.0425 S/m at 25 °C for the gypsum with NaCl in the casting compound was in well accordance with skull conductivity range from 0.03 S/m to 0.08 S/m

measured at 37 °C reported by Hoekema [26]. This gypsum as skull model and other phantom materials presented here established a brain-to-skull conductivity ratios of 1:1/8, in close relation to the ration of 1:1/12 reported by Ostendorp et al. [27].

The reed sticks provided a conductivity anisotropy with transversal to longitudinal direction ratio of approximately 1:3. Within a physical head phantom, reed sticks could be used to model white matter anisotropy. The sticks embody a solid model material not depending on complex support structures. Thus, they can be placed easily inside the compartment of the intracranial volume and used to model an anisotropic internal compartment. The anisotropy ratio of approximately 1:3 implemented by the reed sticks is in good accordance with the ratios of 1:2 and 1:5 often referred to in literature [13, 14], even though this ratio is below the white matter anisotropy ratio of 1:10 reported from earlier measurements [15].

With the materials characterized in the present study, the widely used approximation of the head as volume conductor comprising intracranial volume, skull and scalp [9] can be realized in a physical phantom. The electrolyte conductivity in all analyzed materials is based on a 0.17% NaCl solution. Consequently, the multi-compartment phantom incorporating these materials possesses a practically stationary ion concentration. Thus, the limitation of transient conductivity configurations due to diffusion processes across compartments with varying ion concentration [2, 28, 29] can be overcome.

All materials used to manufacture the samples in this study were commercially available. Using these standardized products and standardized production procedures, we can ensure reproducibility of the phantom production. However, all samples have been manually produced and sample properties, i.e. the area A and the thickness/length d, used in Eq. (2) had tolerances influencing the calculated conductivity values.

The conductivities resulting from measurements with the four-point setup demonstrated high reproducibility with a coefficients of variation (CV) of 0.8% and reliability compared to the measurement results obtained with the ProfiLine Cond 3310 with a deviation of only 0.2%.

The tested materials demonstrate consistent results across several measurement days. Consequently, our produced phantoms can be used for several days in measurement campaigns.

Conclusion

We investigated the applicability of NaCl solution, agar hydrogel and gypsum for modeling intracranial volume, scalp and skull in physical head phantoms for, e.g. EEG, MEG and TES, CDI. Agar hydrogel and gypsum are well-known, moldable materials available at low cost, which are inherently mechanically stable and permeable for ions. Our measurements showed that gypsum provides a stable conductivity barrier allowing for physiologically plausible skull conductivity values interfacing with NaCl solution. With the tested reed sticks, we introduced a potential material for conductivity anisotropy realization in a physical phantom.

Materials And Methods

Sodium chloride solution

For reference purposes, we used NaCl (Sodium chloride ≥ 99%, Carl Roth GmbH + Co. KG, Karlsruhe, Germany) to prepare the electrolyte solutions for providing the charge carrier in the physical head phantom. The conductivity of the sodium chloride solution was tested with a conductivity meter ProfiLine Cond 3310 (Xylem Analytics Germany Sales GmbH & Co. KG, Weilheim, Germany).

Agarose

We applied agarose (Agarose Broad Range, Carl Roth GmbH + Co. KG, Karlsruhe, Germany) as a solidifying agent in the NaCl solution, where higher agarose concentrations yield higher mechanical stability of the synthetic skin. We added 2 wt%, 3 wt% and 4 wt% agarose to the heated electrolyte solution (approx. 65 °C) under constant stirring. The milky dispersion was heated to approx. 80 °C until a clear solution emerged. The agarose electrolyte solution was kept liquid at around 65 °C until poured in the casting mold. After cooling to room temperature, the agarose electrolyte solution formed a mechanically stable hydrogel.

Gypsum

In gypsum, the solid crystal embodies a structural conductivity barrier. We selected Stewaform (Glorex GmbH, Rheinfelden, Germany) as casting compound in order to allow the formation of a realistic skull-shaped compartment. The Stewaform powder was mixed with either deionized water or 0.17% NaCl solution in the ratio of 2:1 to form a casting compound and poured in negative molds of the desired form and let dry at 40 °C for 2 hours. We infiltrated the dried gypsum with an epoxy resin to protect the gypsum structures from dissolution when in contact with the NaCl solutions. We infiltrated the gypsum for one minute in a two components epoxy resin XTC-3D (Smooth-On Inc., Macungie, PA, USA) in a ratio of 2:1 (epoxy resin:hardener). The infiltrated gypsum was again dried at 40 °C for 10 min.

Reed sticks

We fit 80 reed sticks (diffusor sticks, Jörn Poppenhäger, Ottweiler, Germany) into a hollow plastic tube with 29 mm inner diameter. In the middle of the 170 mm long tube, we resected two circular cut-outs. To the four openings of the tube, we attached electrode configurations comprising a pellet electrode (MedCaT GmbH, Munich, Germany) in 2.5 mm and a ring electrode (MedCaT GmbH, Munich, Germany) in 30 mm distance to the tube openings. The tube and electrode configurations were densely sealed and the whole volume was filled with 0.17% NaCl solution.

Impedance measurements

We tested the electrical properties of the material samples including agar hydrogel, gypsum and reed sticks by means of four-point impedance measurements. A Gamry Reference 600 Plus (Gamry Instruments, Warminster, PA, USA) measured the impedance of the cell comprising of the material sample clamped between two NaCl solution compartments with a concentration of 0.17% NaCl in deionized water as depicted in Fig. 8. The NaCl solution compartments held an outer pair of silver/silver-chloride ring electrodes at a distance of 160 mm for impressing an electric current, and an inner pair of silver/silver-chloride electrodes with 4 mm diameter for measuring the resulting potential difference. A more detailed description

of the setup can be found in [21]. The reed sticks were tested in the above-mentioned double tube configuration.

We tested the impedance for three samples of 0.17% NaCl solution, agarose hydrogels with 2 wt%, 3 wt% and 4 wt% agarose and each one gypsum sample with and without 0.17% NaCl solution in the casting compound. The gypsum samples were tested three times in this procedure after they have been dried at ambient air for at least 20 h. Each measurement series contained a frequency spectrum from 0.1 Hz to 100 kHz and an impedance measurement at constant frequency of 1 Hz over 10 min; series were conducted three times with 30 min pause between repetitions.

Further, we tested three samples of agarose hydrogels with 2 wt% agarose and one gypsum with 0.17% NaCl solution in the casting compound on a broader frequency and time scale. Each measurement series contained a frequency spectrum from 0.01 Hz to 100 kHz and an impedance measurement at constant frequency of 10 Hz over 60 min; series were conducted three times with 6 h pause between repetitions.

Simultaneously to the impedances, we measured the temperature in the cell with an electrically insulated stainless steel probe connected to a Traceable® Excursion-Trac (VWR International bvba, Leuven, Belgium).

Conductivity calculation

The impedance measurement Z_{NaCl} of the cell containing NaCl solution only serves as a reference for the temperature compensation according to Eq. 1 and to determine the net impedance of the sample as the difference between the impedance of a cell with and without a material sample.

$$Z_{25} = \frac{Z_{meas} - Z_{NaCl}}{1 + \alpha \cdot (\vartheta_{meas} - 25°C)} \qquad (1)$$

with Z_{25} and Z_{meas} denoting absolute impedance values at 25 °C and measurement, temperature ϑ_{meas} in °C and the linear factor α. The linear factor α, also called cell constant, was determined using the reference impedance measurement of a cell containing 0.17% NaCl solution only. The temperature compensated net impedance Z_{25} was applied in Eq. (2) to calculate the material conductivity:

$$\kappa = \frac{\mathrm{d}}{Z_{25} \cdot \mathrm{A}} \qquad (2)$$

with the material sample thickness/length d and the surface area A. Time traces of conductivity data were quantitatively analyzed, using the ratio between the mean conductivity value and the mean standard deviation, which is defined as signal-to-noise ratio (SNR).

The tube configuration loaded with the reed sticks was measured in longitudinal and transversal direction. For both directions, we calculated the conductivity according to (2) with temperature compensated impedance values from (1). The conductivity anisotropy was calculated as the ratio between longitudinal and transversal conductivity.

Declarations

Ethics approval and consent to participate

Not applicable.

Consent for publication

Not applicable.

Availability of data and materials

All data generated or analyzed during this study are included in this published article.

Competing interests

The authors, AH, RM and JH, declare that they have no competing interests.

Funding

This project has received funding from the European Union's Horizon 2020 research and innovation programme under grant agreement No 686865 (project BREAKBEN), from the Free State of Thuringia under 2017 VF 0035 and 2018 IZN 004 co-financed by the European Union under the European Regional Development Fund (ERDF), from the German Research Foundation under grant number HA 2899/21-1, and from the Carl Zeiss foundation.

Authors' contributions

AH essentially contributed to the conception of the study, the data acquisition, processing and analysis, and the manuscript drafting and revision.

RM essentially contributed to the data acquisition, the interpretation of data and the manuscript revision.

JH essentially contributed to the conception of the study, the interpretation of data, and the manuscript revision.

Acknowledgement

The authors thank Danae Crascovscaia for support during data acquisition.

References

1. Hunold A, Funke ME, Eichardt R, Stenroos M, Haueisen J. EEG and MEG: Sensitivity to epileptic spike activity as function of source orientation and depth. Physiol Meas. 2016;37:1146–62.
2. Wetterling F, Liehr M, Schimpf P, Liu H, Haueisen J. The localization of focal heart activity via body surface potential measurements: Tests in a heterogeneous torso phantom. Phys Med Biol. 2009;54:5395–409.
3. Hömmen P, Mäkinen AJ, Hunold A, Machts R, Haueisen J, Zevenhoven KCJ, et al. Evaluating the Performance of Ultra-Low-Field MRI for in-vivo 3D Current Density Imaging of the Human Head. Front Phys. 2020;8.
4. Hunold A, Haueisen J, Ahtam B, Doshi C, Harini C, Camposano S, et al. Localization of the epileptogenic foci in tuberous sclerosis complex: A pediatric case report. Front Hum Neurosci. 2014;8:1–12.
5. 10.1016/j.brs.2011.10.001
Peterchev AV, Wagner TA, Miranda PC, Nitsche MA, Paulus W, Lisanby SH, et al. Fundamentals of transcranial electric and magnetic stimulation dose: Definition, selection, and reporting practices. Brain Stimul [Internet]. Elsevier Inc; 2012;5:435–53. Available from: http://dx.doi.org/10.1016/j.brs.2011.10.001.
6. Vorwerk J, Cho JH, Rampp S, Hamer H, Knösche TR, Wolters CH. A guideline for head volume conductor modeling in EEG and MEG. Neuroimage [Internet]. Elsevier Inc.; 2014;100:590–607. Available from: http://linkinghub.elsevier.com/retrieve/pii/S1053811914005175.
7. http://dx.plos.10.1371/journal.pone.0093154
Aydin Ü, Vorwerk J, Küpper P, Heers M, Kugel H, Galka A, et al Combining EEG and MEG for the reconstruction of epileptic activity using a calibrated realistic volume conductor model. Barnes GR, editor. PLoS One [Internet]. Public Library of Science; 2014 [cited 2018 Oct 15];9:e93154. Available from: http://dx.plos.org/10.1371/journal.pone.0093154.
8. McCann H, Pisano G, Beltrachini L. Variation in Reported Human Head Tissue Electrical Conductivity Values. Brain Topogr. 2019;32:825–58.
9. Stenroos M, Hunold A, Haueisen J. Comparison of three-shell and simplified volume conductor models in magnetoencephalography. Neuroimage. 2014;94:337–48.
10. Geddes LA, Baker LE. The specific resistance of biological material-A compendium of data for the biomedical engineer and physiologist. Med Biol Eng. 1967;5:271–93.

11. Homma S, Musha T, Nakajima Y, Okamoto Y, Blom S, Flink R, et al. Conductivity ratios of the scalp-skull-brain head model in estimating equivalent dipole sources in human brain. Neurosci Res. 1995;22:51–5.
12. Wendel K, Narra NG, Hannula M, Kauppinen P, Malmivuo J. The influence of CSF on EEG sensitivity distributions of multilayered head models. IEEE Trans Biomed Eng. 2008;55:1454–6.
13. Güllmar D, Haueisen J, Reichenbach JR. Influence of anisotropic electrical conductivity in white matter tissue on the EEG/MEG forward and inverse solution. A high-resolution whole head simulation study. Neuroimage. 2010;51:145–63.
14. Wolters CH, Anwander A, Tricoche X, Weinstein D, Koch MA, MacLeod RS. Influence of tissue conductivity anisotropy on EEG/MEG field and return current computation in a realistic head model: A simulation and visualization study using high-resolution finite element modeling. Neuroimage [Internet]. Academic Press; 2006 [cited 2018 Nov 2];30:813–26. Available from: https://www.sciencedirect.com/science/article/pii/S1053811905007871.
15. Nicholson PW. Specific impedance of cerebral white matter. Exp Neurol. 1965;13:386–401.
16. Baillet S, Rira JJ, Main G, Magin JF, Aubert J, Ganero L. Evaluation of inverse methods and head models for EEG source localization using a human skull phantom. Phys Med Biol [Internet]. 2001;46:77–96. Available from: http://www.ncbi.nlm.nih.gov/entrez/query.fcgi?cmd=Retrieve&db=PubMed&dopt=Citation&list_uids=11197680.
17. Leahy RM, Mosher JC, Spencer ME, Huang MX, Lewine JD. A study of dipole localization accuracy for MEG and EEG using a human skull phantom. Electroencephalogr Clin Neurophysiol. 1998;107:159–73.
18. 10.1016/j.brs.2015.06.009%5Cnpapers3://publication/doi/10.1016/j.brs.2015.06.009 Kim D, Jeong J, Jeong S, Kim S, Jun SC, Chung E. Validation of computational studies for electrical brain stimulation with phantom head experiments. Brain Stimul [Internet]. Elsevier Inc.; 2015;8:914–25. Available from: http://dx.doi.org/10.1016/j.brs.2015.06.009%5Cnpapers3://publication/doi/10.1016/j.brs.2015.06.009.
19. Jung Y-J, Kim J-H, Kim D, Im C-H. An image-guided transcranial direct current stimulation system: a pilot phantom study. Physiol Meas [Internet]. 2013;34:937–50. Available from: http://stacks.iop.org/0967-3334/34/i=8/a=937?key=crossref.d74fe62408c40afdd46c161acec4f413.
20. Liehr M, Haueisen J. Influence of anisotropic compartments on magnetic field and electric potential distributions generated by artificial current dipoles inside a torso phantom. Phys Med Biol. 2008;53:245–54.
21. Hunold A, Strohmeier D, Fiedler P, Haueisen J. Head phantoms for electroencephalography and transcranial electric stimulation: A skull material study. Biomed Tech. 2018;63:647–55.
22. Lide DR. CRC Handbook of Chemistry and Physics, 93rd Edition. In: Haynes WM, Lide DR, Bruno TJ, editors. Handb Chem Phys [Internet]. CRC Press; 2012. p. 5–73. Available from: https://books.google.com/books?hl=fr&lr=&id=-BzP7Rkl7WkC&pgis=1.
23. Burger HC, Milaan, van JB. Measurements of the specific Resistance of the human Body to direct Current. Acta Med Scand. 1943;114:584–607.
24. Fiedler P, Muhle R, Griebel S, Pedrosa P, Fonseca C, Vaz F, et al. Contact Pressure and Flexibility of Multipin Dry EEG Electrodes. IEEE Trans Neural Syst Rehabil Eng. 2018;26:750–7.

25. Tang C, You F, Cheng G, Gao D, Fu F, Yang G, et al. Correlation between structure and resistivity variations of the live human skull. IEEE Trans Biomed Eng. 2008;55:2286–92.
26. Hoekema R, Wieneke GH, Leijten FSS, Van Veelen CWM, Van Rijen PC, Huiskamp GJM, et al. Measurement of the conductivity of skull, temporarily removed during epilepsy surgery. Brain Topogr. 2003;16:29–38.
27. Oostendorp TF, Delbeke J, Stegeman DF. The conductivity of the human skull: Results of in vivo and in vitro measurements. IEEE Trans Biomed Eng. 2000;47:1487–92.
28. 10.1007/s10439-009-9799-6
Sadleir RJ, Neralwala F, Te T, Tucker A. A Controllably Anisotropic Conductivity or Diffusion Phantom Constructed from Isotropic Layers. Ann Biomed Eng [Internet]. Springer US. 2009 [cited 2018 Oct 19];37:2522–31. Available from: http://link.springer.com/10.1007/s10439-009-9799-6.
29. Tenner U, Haueisen J, Nowak H, Leder U, Brauer H. Source localization in an inhomogeneous physical thorax phantom. Phys Med Biol [Internet]. IOP Publishing; 1999 [cited 2018 Oct 19];44:1969–81. Available from: http://stacks.iop.org/0031-9155/44/i=8/a=309?key=crossref.4b006336a866caad04db7e7e10705853.

Figures

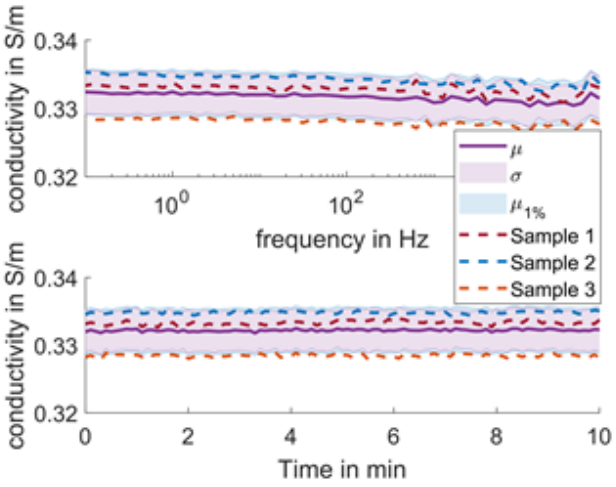

Figure 1

Conductivity data at 25 °C averaged from three samples of 0.17 % NaCl solution over frequency spectrum (top) and at 1 Hz over time (bottom). Samples were tested in three measurement series comprising an impedance frequency spectrum from 0.1 Hz to 100 kHz (top) and an impedance test at a constant frequency of 1 Hz over 10 min (bottom). Dashed lines represent the averaged data from the three measurement series for the three color-coded samples. Shaded areas represent the standard deviation (σ) and 1 % deviation from the mean (μ1%).

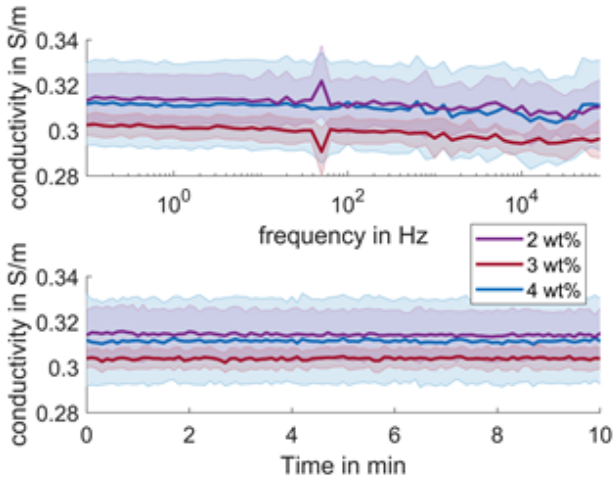

Figure 2

Figure 2 Conductivity data at 25 °C averaged from each three samples with of 2 wt%, 3 wt% and 4 wt% (color-coded) agar in 0.17 % NaCl solution over frequency spectrum (top) and at 1 Hz over time (bottom). Agar hydrogel samples were tested in three measurement series comprising an impedance frequency spectrum from 0.1 Hz to 100 kHz (top) and an impedance test at a constant frequency of 1 Hz over 10 min (bottom). Solid lines indicate the mean value (μ) and shaded areas represent the standard deviation (σ). Even though measurements were conducted in a grounded faraday cage, the spectra showed a deviation at 50 Hz reflecting power-line interference.

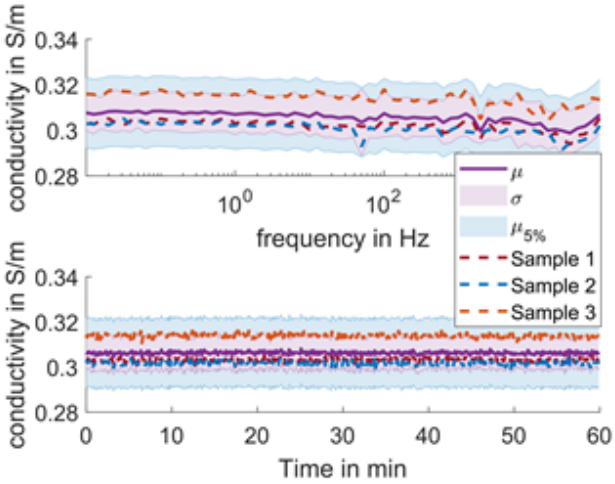

Figure 3

Conductivity data at 25 °C averaged from three samples (color-coded) of 2 wt% agar in 0.17 % NaCl solution over frequency spectrum (top) and at 10 Hz over time (bottom). Samples were tested in three measurement series comprising an impedance frequency spectrum from 0.01 Hz to 100 kHz (top) and an impedance test at a constant frequency of 10 Hz over 60 min (bottom). Shaded areas represent the standard deviation (σ) and 1 % deviation from the mean (μ1%).

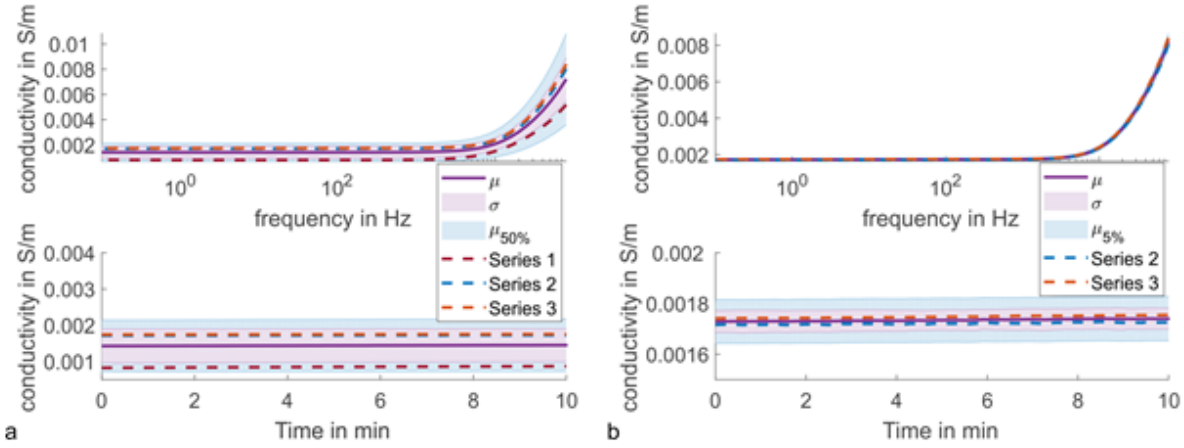

Figure 4

Conductivity data at 25 °C of the gypsum sample without NaCl in the casting compound averaged across measurement series 1–3 (a) and 2, 3 (b) over frequency (top) and time (bottom). The Stewaform gypsum sample was tested in three measurement series comprising an impedance frequency spectrum from 0.1 Hz to 100 kHz (top) and an impedance test at a constant frequency of 1 Hz over 10 min (bottom). Labels indicate mean value (μ), standard deviation (σ) and 50 % or 5 % range from the mean value (μ50% or μ5%).

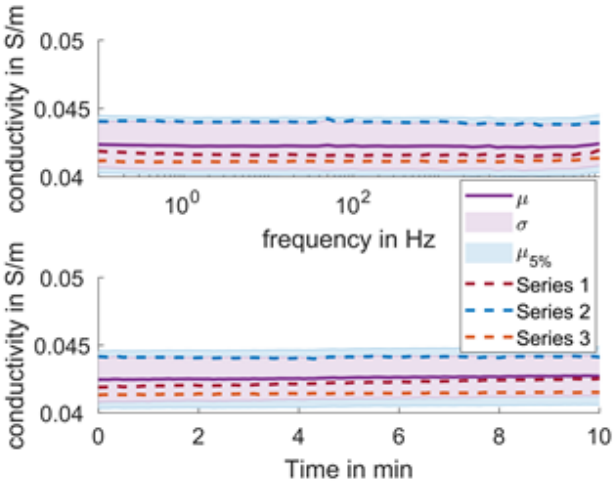

Figure 5

Conductivity data at 25 °C of the gypsum sample with NaCl in the casting compound averaged across measurement series (color-coded dashed lines) over frequency (top) and time (bottom). The Stewaform gypsum sample was tested in three measurement series comprising an impedance frequency spectrum from 0.1 Hz to 100 kHz (top) and an impedance test at a constant frequency of 1 Hz over 10 min (bottom). Labels indicate mean value (μ), standard deviation (σ) and 5 % range from the mean value (μ5%).

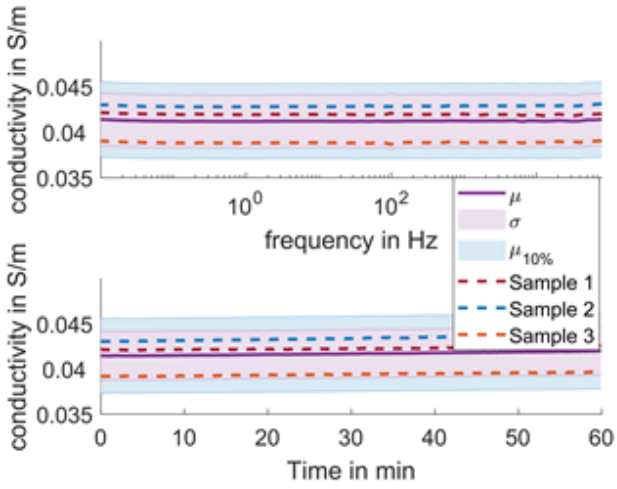

Figure 6

Conductivity data at 25 °C averaged from three samples (color-coded) of gypsum with NaCl in the casting compound averaged over frequency spectrum (top) and at 10 Hz over time (bottom). Samples were tested in three measurement series comprising an impedance frequency spectrum from 0.01 Hz to 100 kHz (top) and an impedance test at a constant frequency of 10 Hz over 60 min (bottom). Shaded areas represent the standard deviation (σ) and 10 % deviation from the mean (μ10%).

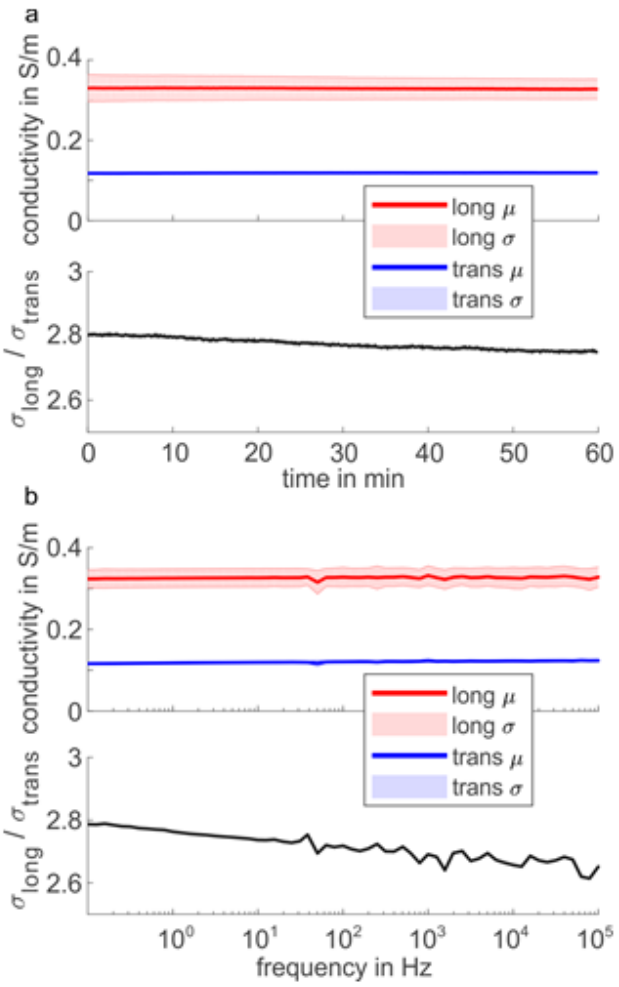

Figure 7

Conductivity data at 25 °C (top) and calculated anisotropy ratios (bottom) of the cell with reed sticks averaged over time (a) and frequency (b). The reed sticks were tested in five measurement series comprising an impedance test at a constant frequency of 10 Hz over 1 hour (a) and an impedance frequency spectrum from 0.1 Hz to 100 kHz (b). Labels indicate mean value (μ), standard deviation (σ).

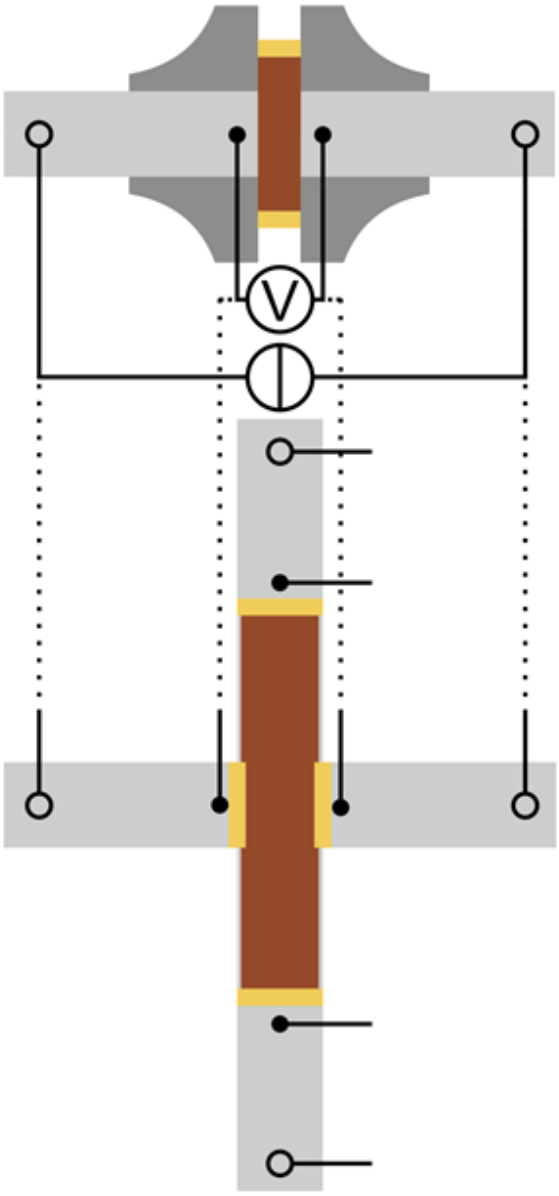

Figure 8

Measurement schemes for isotropic (top) and anisotropic (bottom) impedance measurements. The cell with a material sample (brown) in plastic tubes filled with NaCl solution (light gray) incorporates the paired measurement electrodes (black filled dots) with the outer electrode pair (black outlined dots) for current application, both being integrated into the Gamry Reference 600 Plus impedance analyzer. Sealing rings (yellow) and POM flanges (dark gray) complete the setup. Adopted from [21].